J. Mater. Environ. Sci. 7 (1) (2016) 337-346
ISSN : 2028-2508
CODEN: JMESCN

New hydrazine derivatives as corrosion inhibitors for mild steel protection in phosphoric acid medium. Part A: Experimental study

M. E. Belghiti[1], S. Tighadouini[1], Y. Karzazi[1,2], A. Dafali[*1], B. Hammouti[1], S. Radi[1], R. Solmaz[3*]

[1]*Laboratory of Applied Chemistry and Environment (URAC-18), Faculty of Sciences, University of Mohammed Premier, B.P. 4808, 60046 Oujda, Morocco.*

[2] *National School of Engineering and Applied Sciences (ENSA), University of Mohammed Premier, B.P. 3, 32003 Sidi Bouafif, Al Hoceima, Morocco.*

[3,*]*Bingöl University, Science and Letters Faculty, Chemistry Department, 12000 Bingöl, Turkey*

Received 22 Mar 2015, Revised 20 Sept 2015, Accepted 25 Sept 2015
[*] *E-mail: dafali2@yahoo.fr & rsolmaz01@gmail.com*

Abstract

The inhibitory effects of three hydrazine derivatives, namely 1,2-bis(pyrrol-2-ylidenemethyl)hydrazine (HZ1), 1,2-bis(thiophen-2-ylidenemethyl)hydrazine (HZ2) and 1,2-Bis(furyl-2-ylidenmethyl)hydrazine (HZ3) for the corrosion of mild steel in phosphoric acid solution was studied using weight loss (WL), electrochemical impedance spectroscopy (EIS) and polarization curves (PC). It was found that the inhibition efficiency of the compounds increases with the increasing their concentration. The adsorption of inhibitors on the steel surface follows the Langmuir isotherm. The effect of temperature on the corrosion behavior of mild steel in phosphoric acid solution in the absence and presence of the inhibitors was also studied. From the experimental data, some thermodynamic parameters were calculated and discussed. Polarization curves showed that HZ1, and HZ3 behave as mixed type corrosion inhibitors in phosphoric acid solution.

Keywords: Hydrazine derivatives, corrosion, mild steel, phosphoric acid.

1. Introduction

Protecting metals against corrosion has widely attracted the interest of scientific researches. Several approaches have been proposed and implemented to protect metals against corrosion. Most commonly, these approaches use inorganic or organic corrosion inhibitors, which reduces the corrosion rate of materials by adsorbing on the metal surfaces. A number of compounds which have N atoms in their aromatic or long carbon chain have been reported as effective corrosion inhibitors [1]. Inhibitory effects are reinforced by the presence of heteroatoms such as S, O and N atoms. The presence of these atoms in molecular structure facilitates their adsorption on the metal surface in the sequence of S>N>O [2-4].

The N-containing heterocyclic compounds generally perform their inhibition action by adsorbing on metal surfaces through heteroatom. Adsorption of organic compounds on metals surfaces depends on the electronic structure of molecules, steric factors, aromaticity and electron density at donor atoms, presence of functional groups such as –C-O-C-, –C-NH-C-, –C-S-C- and C-N=N-C in their molecular structure, the size and molecular weight of molecule, temperature and electrochemical potential at the metal/solution interface [5-12]. Hydrazine derivatives constitute important classes of organic heterocyclic compounds that have found wide utility in organic synthesis [13,14]. The chemistry of carbon nitrogen double bond of hydrazones (R_1R_2=C=N-NH_2) is becoming the backbone of condensation reaction in benzo-fused heterocyclics [14] and also it constitutes an important class of compounds for developing new drugs [15].

The studied hydrazine derivatives in this work were synthesized and analyzed in our laboratory. The molecular structures of the inhibitors are shown in Figure 1. This present work is designed to correlate the observed inhibition competence with the quantum chemical parameters of the inhibitors that will be treated in next Part B.

1,2-bis(pyrrol-2-ylidenemethyl)hydrazine (HZ1)	1,2-bis(thiophen-2-ylidenemethyl)hydrazine (HZ2)	1,2-Bis(furyl-2-ylidenmethyl)hydrazine (HZ3)
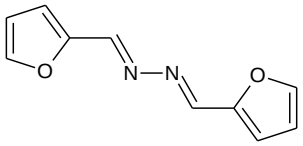	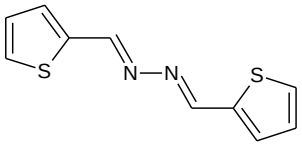	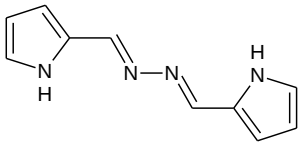

Figure 1: The Molecular structures of hydrazine derivatives.

2. Materials and methods

2.1. Synthesis procedure of the hydrazine derivatives

A series of hydrazine derivatives (Figure 1) were synthesized with high yields according to following simple steps. Hydrazines (15.62mmol) were added to a solution of each heterocycle-2-carbaxaldehyde (31.24mmol) in dry ether (20mL). Then, a few drops of glacial acetic acid were added as catalyst. The mixture was stirred at room temperature for 3 days. The formed products were filtered and washed with dry ether. Structures of the compounds were confirmed by spectral studies.

1,2-bis(furan-2-ylmethylene)hydrazine, HZ1: Yellow powder. Yield 85%.Mp =113°C. R_f = 0.33 (silica/CH_2Cl_2) ^{1}H NMR (300MHz, $CDCl_3$) δ ppm: 8.59 (s, 2H, H_{imine}); 7.62 (d, 2H, H_α); 7.03 (d, 2H, H_γ); 6.63 (m, 2H, H_β). ^{13}C NMR (75 MHz, $CDCl_3$) δ ppm: 150.76 (2C, C_{imine}); 148.14 (2C, furan-C_δ); 146.56 (2C, furan-C_α); 0118.20 (2C, furan-C_Υ); 112.58 (2C, furan-C_β). m/z (M^+):189. IR: ν(CH=N, imine) = 1630 cm^{-1}.

1,2-bis(thiophen-2-ylmethylene)hydrazine, HZ2: Yellow powder. Yield 64%.Mp = 167°C. R_f =0.76 (silica/CH_2Cl_2) ^{1}H NMR (300MHz, DMSO) δ ppm: 8.82 (s, 2H, H_{imine}); 7.76 (d, 2H, H_α), 7.61 (d, 2H, H_γ); 7.18 (t, 2H, H_β). ^{13}C NMR (75 MHz, DMSO) δ ppm: 156.26 (2C, C_{imine}); 138.87 (2C, thiophen-C_δ); 134.25 (2C, thiophen-C_α) ; 131.45 (2C, thiophen-C_β) ; 128.75 (2C, thiophen-C_γ). m/z (M^+): 121.02. IR: ν(CH=N, imine) = 1609cm^{-1}.

1,2-bis(1H-pyrrol-2-ylmethylene)hydrazine,HZ3: Yellow powder. Yield 62%.Mp = 186°C. Rf =0.32 (silica/CH_2Cl_2). ^{1}H NMR (300MHz, DMSO) δ ppm: 11.52 (s, 1H, pyrrole-NH); 8.36 (s, 2H, H_{imine}); 6.96 (d, 2H, H_α); 6.59 (s, 2H, H_γ); 6.16 (m, 2H, H_β). ^{13}C NMR (75 MHz, DMSO) δ ppm: 151.03 (2C, C_{imine}); 127.81 (2C, pyrrole-C_δ) ; 123.71 (2C, pyrrole-C_γ) ; 115.25 (2C, pyrrole-C_β) ; 110.14 (2C, pyrrole-C_α). m/z (M^+):187.08. IR: ν(CH=N, imine) = 1616cm^{-1}.

2.2. Weight loss measurements

Prior to all measurements, the steel samples (0.09%P, 0.38%Si, 0.01%Al, 0.05%Mn, 0.21%C, 0.05%S and the remainder iron) were abraded with a series of emery papers from 400 to 1200 grids. The specimens were washed thoroughly with bi-distilled water degreased with acetone and dried.

Gravimetric experiments were performed according to the standard methods [16]. Weight loss measurements were carried out in a double-walled glass cell. The solution volume was 100 cm^3. Temperature of the solution was 308 K which was controlled thermostatically. The weight loss of mild steel in 2M H_3PO_4 with and without the addition of inhibitor was determined after immersion in acid for 4h. The steel specimens used for these tests had a rectangular form (15mm × 15mm × 1mm).

2.3. Electrochemical measurements

The electrochemical measurements were carried out using a Volta lab (Tacussel- Radiometer PGZ 100) potentiostate and controlled by Tacussel corrosion analysis software model (Voltamaster 4). The corrosion cell was a conventional three-electrode electrolysis cylindrical Pyrex glass cell. The working electrode (WE) had the form of a disc which was cut form a steel sheet. The exposed surface area to the corrosive solution was 1cm^2. A saturated calomel electrode (SCE) and a platinum electrode were used as reference and auxiliary electrodes, respectively. Before recording the polarization curves, the working electrode was initially immersed into the test solution for 30 min to attain its open circuit potential (E_{ocp}). The steel electrode was pre-polarized at -800 mV for 10 min. The polarization curves were obtained from -800 mV to more positive potentials. The test solution was de-aerated with pure nitrogen. Gas bubbling is maintained through the experiments. All potentials were refereed to SCE reference electrode. The test solutions were thermostatically controlled at 308 ± 0.5 K.

Electrochemical impedance spectroscopy (EIS) measurements were carried out at E_{ocp} after obtaining steady-state condition between the frequency ranges of 100 kHz to 10 mHz with a sine wave voltage (10 mV) peak to peak. The EIS data were given in Nyquist representation.

3. Resultants and discussion

3.1. Electrochemical Impedance Measurements

Nyquist plots of mild steel in inhibited and uninhibited acidic solutions containing various concentrations of HZ1, HZ2 and HZ3 are shown in Figure 2a, 2b and 2c, respectively. The polarization resistances, R_p were calculated from the difference in real impedance scale at lower and higher frequencies, as suggested by *Tsuru and al.*[17]. The C_{dl} values were obtained from the following equation:

$$C_{dl} = \frac{1}{2\pi f_{max} R_t} \quad (1)$$

Where, f_{max} is the frequency at which the imaginary component of the impedance ($-Z_{max}$) is maximum. The inhibition efficiency (η %) from the charge transfer resistance was calculated using the following equation:

$$\eta_{Rp}(\%) = \frac{R_{p(inh)} - R_p}{R_{p(inh)}} \quad (2)$$

Where, $R_{p(inh)}$ and R_p are the polarization resistance in the presence and in the absence of inhibitors, respectively. The impedance parameters calculated from the polarization data are given in Table 1.It is seen that R_p values increase with the increase in inhibitor concentration which indicates a protective film formation over the steel surface.

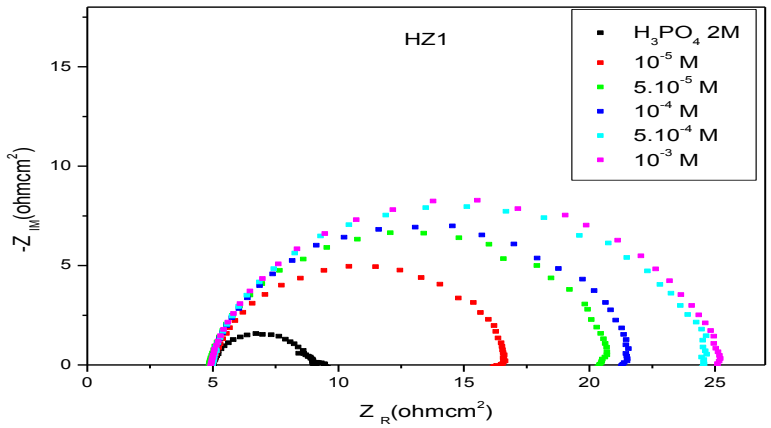

Figure 2a: Nyquist plots of mild steel in 2 M H_3PO_4 without and with different concentrations of HZ1at 308K.

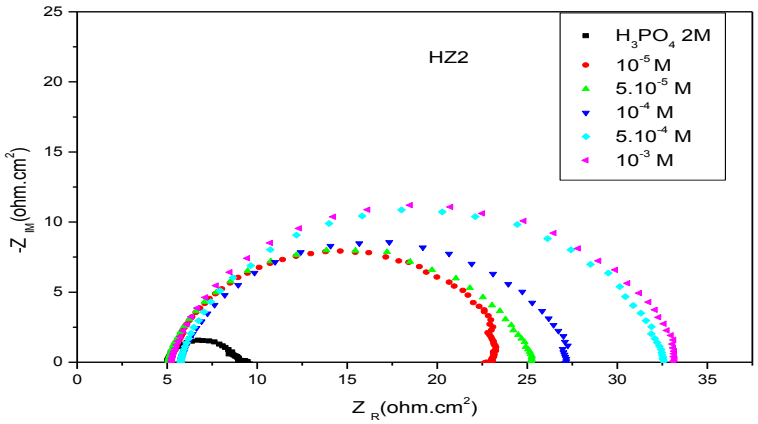

Figure 2b: Nyquist plots of mild steel in 2 M H_3PO_4 without and with different concentrations of HZ2 at 308K.

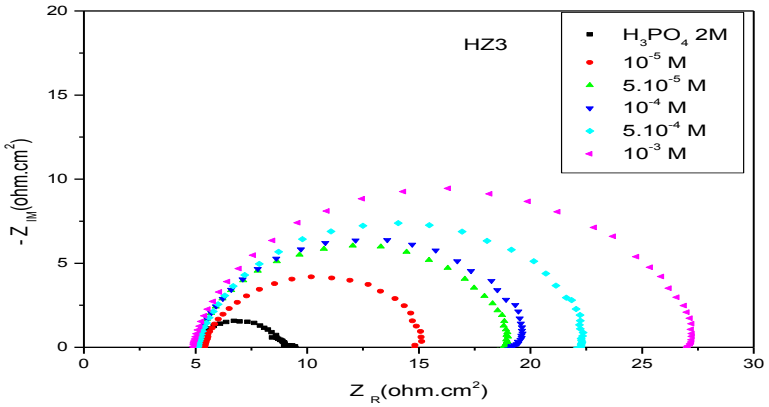

Figure 2c: Nyquist plots of mild steel in 2 M H_3PO_4 without and with different concentrations of HZ3 at 308K.

The double layer capacitance C_{dl} is expressed in the Helmoltz model by:

$$C_{dl} = \frac{\varepsilon_0 \times \varepsilon}{\delta} \quad (3)$$

Where, δ is the thickness of the deposit or film, S is the surface of the electrode, ε_0 is the permittivity of air and ε is the dielectric constant of medium. The decrease in C_{dl} could be explained either by a decrease in local dielectric constant ε [18] and/or by the thickness of the adsorbed layer of the inhibitor on the metal surface [19]. From Table 1, it is clear that the R_p increases whereas the C_{dl} decreases with increasing inhibitor concentration. These results indicate a decrease in the active surface area caused by the adsorption of the inhibitors on the mild steel surface, which reduces corrosion rate. The highest inhibition efficiency (85.6%) was obtained for HZ2 at 10^{-3}M.

Table 1: Corrosion parameters obtained from impedance measurements for mild steel in 2 M phosphoric acid without and with the addition of various concentrations of the hydrazine derivatives.

Inhibitor	Conc. (M)	R_p (Ωcm^2)	f_{max} (Hz)	C_{dl} ($\mu F/cm^2$)	η_{R_P} (%)	θ
Blank	2	04.18	250.00	152.30		
HZ1	10^{-5}	12.01	200.00	65.77	65.94	0.6594
	5.10^{-5}	16.26	158.23	61.86	74.85	0.7485
	10^{-4}	17.00	158.23	59.67	75.94	0.7594
	5.10^{-4}	19.88	158.23	50.60	79.43	0.7943
	10^{-3}	20.44	158.23	49.21	79.50	0.7950
HZ2	10^{-5}	18.88	125.00	67.44	78.33	0. 7833
	5.10^{-5}	20.02	125.00	63.60	79.57	0.7957
	10^{-4}	21.80	125.00	58.40	81.24	0.8124
	5.10^{-4}	26.90	125.00	47.33	84.79	0.8479
	10^{-3}	28.34	125.00	44.93	85.57	0.8557
HZ3	10^{-5}	11.38	250.00	55.94	63.27	0. 6327
	5.10^{-5}	15.50	125.00	82.14	73.61	0.7361
	10^{-4}	17.74	125.00	71.77	76.94	0.7694
	5.10^{-4}	24.56	100.00	64.80	83.35	0.8335
	10^{-3}	27.15	100.00	58.62	84.93	0.8493

The Nyquist diagrams presented in Figure 2 were not perfect semicircles which could be attributed to frequency dispersion [20–22]. It is noteworthy that the best fit of the experimental data is obtained using constant phase elements (*CPE*) which has frequency dispersion rather than capacitances. Based on the values of the electric elements and parameters obtained in them, capacitances were assessed in accordance with the method described by *Hsu and Mansfeld* [22]. *CPE* is a generalized tool, which can reflect exponential distribution of the parameters of the electrochemical reaction related to energetic barrier at charge and mass transfer, as well as impedance behavior caused by fractal surface structure. On the other hand there are some cases where the *CPE* is a formal approximation of the system, having very complicated parameter distribution and it is not possible to give some consistent physical interpretation [21].
The results can be interpreted also in terms of equivalent circuit of the electrical double layer which has been used to model the metal–acidic solution interface [23]. As it can be seen from Figure 2, Nyquist plots are depressed into the real axis and not perfect semicircles as expected from the theory of EIS, which is generally attributed to the inhomogeneity of the metal surface arising from surface roughness or interfacial phenomena [24-25].

3.2. Polarization measurements

The polarization curves of the steel in phosphoric acid solution in the absence and presence of hydrazine derivatives at different concentrations at 308K are presented in Figure 3a, 3b and 3c, respectively

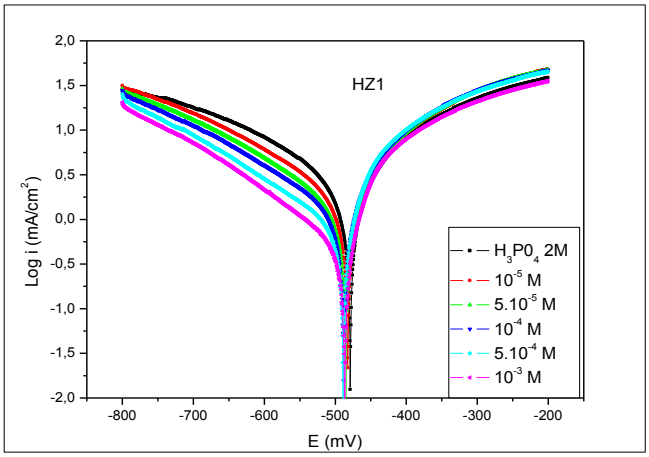

Figure 3a: Polarization curves of mild steel in 2 M H_3PO_4 solution without and with different concentrations of HZ1.

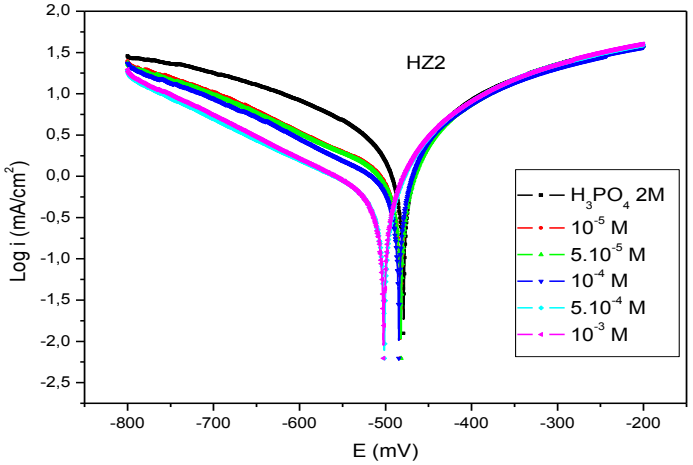

Figure 3b: Polarization curves of mild steel in 2 M H_3PO_4 solution without and with different concentrations of HZ2.

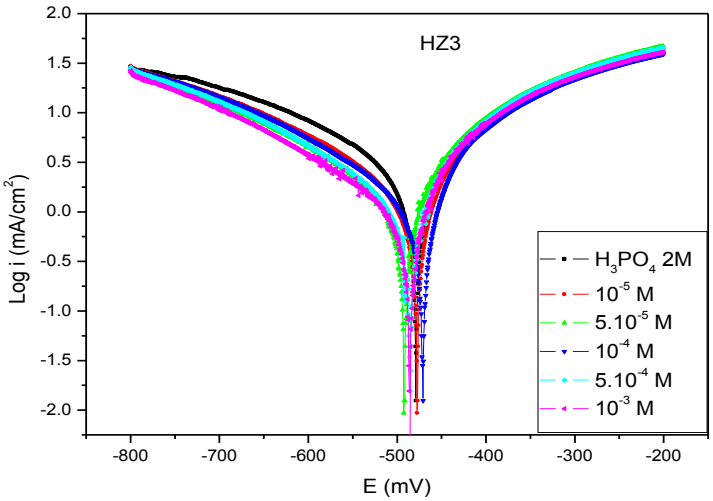

Figure 3c: Polarization curves of mild steel in 2 M H_3PO_4 solution without and with different concentrations of HZ3.

The calculated electrochemical parameters from the polarization measurements such the corrosion potentials (E_{corr}), corrosion current densities (i_{corr}), cathodic Tafel slopes (β_c) and percentage inhibition efficiencies (η_I %) are shown in Table 2. The inhibition efficiencies were calculated from the polarization curves using following equation (η_I %):

$$\eta_I(\%) = \frac{i^0_{corr} - i_{corr}}{i^0_{corr}} \quad (4)$$

Where, i^o_{corr} and i_{corr} are uninhibited and inhibited corrosion current densities, respectively.

Table 2: Electrochemical parameters of mild steel determined from polarization curves obtained in 2 M phosphoric acid at various concentrations of hydrazine derivatives at 308K.

Inhibitors	Conc. (M)	$-E_{corr}$ (mV)	$-\beta_C$ (mV/dec)	i_{corr} (mA/cm^2)	η (%)	θ
Blank	2	480	237.6	2.9790	…..	…..
HZ1	10^{-5}	480	212.3	1.7020	61.48	0.6148
	5.10^{-5}	480	196.7	1.2823	70.97	0.7097
	10^{-4}	485	213.8	1.2180	72.43	0.7243
	5.10^{-4}	485	191.8	0.7490	83.05	0.8305
	10^{-3}	480	183.8	0.5239	88.14	0.8814
HZ2	10^{-5}	480	190.9	0.8286	81.39	0.8139
	5.10^{-5}	480	194.2	0.8227	81.52	0.8152
	10^{-4}	485	184.8	0.6724	84.90	0.8490
	5.10^{-4}	510	198.4	0.4923	88.79	0.8879
	10^{-3}	510	184.2	0.4713	89.42	0.8942
HZ3	10^{-5}	480	254.5	1.0490	62.78	0.6278
	5.10^{-5}	490	239.6	1.5737	64.65	0.6465
	10^{-4}	470	209.7	1.0969	75.36	0.7536
	5.10^{-4}	485	193.8	0.7195	83.84	0.8384
	10^{-3}	485	177.3	0.5120	88.50	0.8850

It is clearly seen from Table 2 and Figure 3 that i_{corr} decreases in the presence of the inhibitors and this increase pronounced more and more when the concentration of the inhibitors increased. The maximum η % was obtained at 10^{-3} M for HZ2. The inhibitory actions of the hydrazines were classified as HZ2 > HZ3 > HZ1.
The characteristics of the polarization curves revealed that hydrazines act as mixed-type with predominantly cathodic type since the E_{corr} values in the inhibited solutions were almost unchanged, whereas corrosion rates, especially cathodic current densities, were reduced significantly. This observation means that hydrazine molecules act on cathodic sites to block the reduction of hydrogen ions to mild steel surface. The cathodic and anodic current- potential curves almost gave rise to parallel Tafel lines indicating that the hydrogen evolution and metal dissolution reactions were activation-controlled and the reaction mechanisms were not affected by the presence of the inhibitors [26-29]. Only slight changes were observed in the cathodic Tafel slope (βc), which suggests that the inhibiting action occurred by simple blocking of the available cathodic sites on the metal surface. Blocking active surface area of the steel leads to a decrease in the exposed surface area necessary for hydrogen evolution.
The electrochemical experiments revealed that HZ2 acts as best corrosion inhibitor among the tested hydrazine derivatives. The presence of additional two sulfur atoms in the molecular structure of HZ2 should contributed an enhanced inhibitory efficiency. The efficiency decreases when two sulfur atoms substitute by two nitrogen atoms (HZ3) and the nitrogen by oxygen in HZ1. Thus the inhibitors performed inhibitory action in the order of S> N> O.

3.4. Effect of temperature

Temperature may effects kinetics of corrosion. To examine the effect of temperature on the corrosion inhibition effects of the inhibitors, weight loss (WL) experiments were made in the temperature range from 308K to 328K. The tests were performed after immersing the steel to the aggressive solution in the presence of the optimum inhibitor concentration (10^{-3}M) for 1 h. The similar tests were repeated in the absence of the inhibitors for comparison. The corresponding data are shown in Table 3. From the WL measurements, the corrosion rate (W_{corr}), the inhibition efficiency (η_w %) of the inhibitors and the degree of surface coverage (θ) were calculated using the following equations [30]:

$$\eta_W(\%) = \frac{W^0_{corr} - W_{corr}}{W^0_{corr}} \times 100 \quad (5)$$

$$\theta = \frac{W^0_{corr} - W_{corr}}{W^0_{corr}} \quad (6)$$

Where, W_{corr} and W^o_{corr} are the weight losses for mild steel in phosphoric acid solution in the presence and absence of the inhibitors, and θ is the degree of surface coverage of the inhibitors. From the results, it was found that HZ1, HZ2 and HZ3, adsorb on the steel surface at all temperatures and corrosion rates increases in absence and presence of the inhibitors. The increase in the absence of the inhibitors was more dominant most probably due to the excess dissolution of metal which also cause increase in active surface area.

Table 3: Corrosion parameters calculated from weight loss measurements for mild steel in 2 M phosphoric acid in the absence and presence of HZ1, HZ2 and HZ3 (10^{-3}M) at various temperatures.

	308K		318K		328K	
Inhibitor	W_{corr} (mg/cm^{2}h)	η_W (%)	W_{corr} (mg/cm^{2}h)	η_W (%)	W_{corr} (mg/cm^{2}h)	η_W (%)
Blank	4.1322	…..	9.0778	…..	15.39	…..
HZ1	0.93	77.40	1.68	70.79	2.901	65.11
HZ2	0.73	82.49	3.58	81.49	7.702	81.10
HZ3	0.77	81.37	3.14	65.41	6.34	58.82

3.5. Adsorption isotherm and thermodynamic parameters

The establishment of adsorption isotherms that describe the adsorption of a corrosion inhibitor can provide important clues to the nature of the metal-inhibitor interaction. Adsorption of the organic molecules occurs as the interaction energy between molecule and metal surface is higher than that between the water molecule and

the metal surface [31]. In order to obtain the adsorption isotherm, the degree of surface coverage (θ) for various concentrations of the HZ1, HZ2 and HZ3 has been calculated at 303 K from impedance data by the ratio η_{R_P}(%)/100. The results obtained for the three inhibitors tested in 2 M H_3PO_4 solution fit well Langmuir adsorption isotherm given by Eq. (7) (Figure 4).

$$\frac{C}{\theta} = \frac{1}{K_{ads}} + C \tag{7}$$

K_{ads} is the equilibrium constant for the adsorption-desorption process. A plot of C/θ versus C_{inh} yields straight line with slopes approaching to 1. The linear correlation coefficients are close to 1.
The standard free energy of adsorption, ($\Delta G°_{ads}$) on the mild steel surface is related to K_{ads} with the equation (8) given below:

$$\Delta G^0_{ads} = -RT \ln(55{,}55 \times K_{ads}) \tag{8}$$

Where, R is the gas constant (8.314J/Kmol), T is the absolute temperature (K), and the value of 55.55 is the concentration of water in the solution in M. ΔG°_{ads}, K and R^2 of HZ1, HZ2 and HZ3 were calculated from impedance data and are given in Table 4. We remark that the best fit was obtained with the Langmuir isotherm (Figure 4), the slopes of HZ1, HZ2 and HZ3 are too close to unity (1.006 of HZ1, 1.014 of and 1.001 of HZ3) with (R^2= 0.9997 of HZ1, R^2=1 of and R^2=0.9993 of HZ3). Also, the values of K_{ads} follow the order of HZ2 > HZ3 > HZ1. Generally, large value of K_{ads} means better inhibition performance of a given inhibitor. This is in good agreement with the values of η_W obtained in Table 3.

Table 4: Adsorption parameters of HZ1, HZ2 and HZ3 on mild steel in 2M phosphoric acid solution at 308K

Inhibitor	R^2	$K_{ads}(M^{-1})$	Slopes	ΔG°_{ads} (kJ/mol)
HZ1	1.0000	+22217	1.014	-35.91
HZ2	0.9991	+55280	1.006	-38.25
HZ3	0.9993	+54274	1.001	-38.20

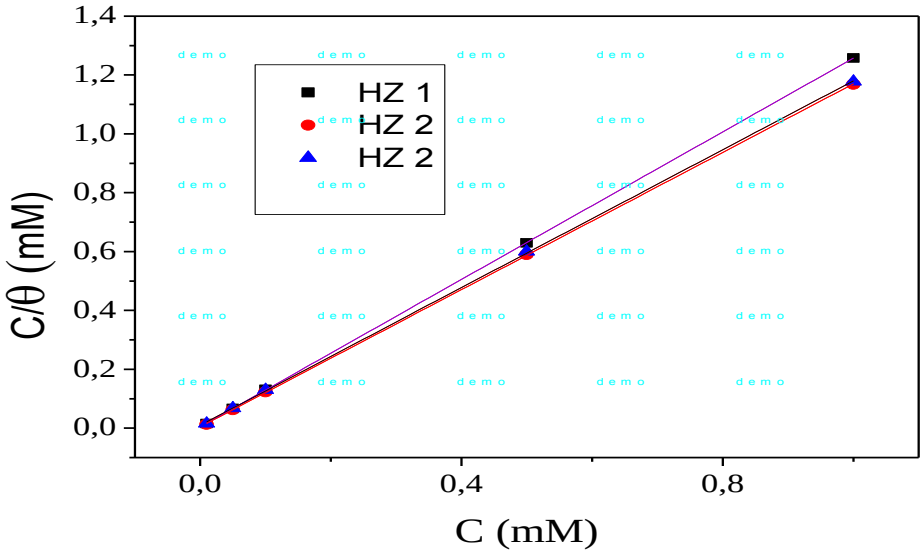

Figure 4: Langmuir isotherms adsorption model of HZ1, HZ2 and HZ3 on mild steel surface in 2M H_3PO_4 solution at 308K.

The values of ΔG°_{ads} < 0 indicate spontaneous adsorption of the organic molecules on metallic surface. The $\Delta G°_{ads}$ are negative and high indicate the strong interactions between the inhibitor molecules and the metal surface [32, 33]. Generally, the ΔG°_{ads} values of -20 kJ/mol or less negative are associated with physical

adsorption; those of -40 kJ/moL or more negative involves charge sharing or transfer from the inhibitor molecules to the metal surface to form a coordinate covalent bond (chemisorption) [34, 35]. In the present study, the obtained values of ΔG°_{ads} closed to -40kJ/moL (Table 4). Therefore, it is concluded that both physical and chemical interactions occur. But, chemical interactions should be dominant for the adsorption of the hydrazine molecules on the mild steel surface [36-39].

Conclusions

- Three hydrazine derivatives, HZ1, HZ2 and HZ2, act as good inhibitors for the corrosion of mild steel in 2M H_3PO_4 solution. Inhibition efficiency increases with the increasing inhibitor concentration, and reaches maximum values of 88.14% (HZ1), 89.42% (HZ2) and 88.50% (HZ3) at 10^{-3} M.
- The inhibition efficiencies of the tested inhibitors follows the order of HZ2 > HZ3 > HZ1.
- The adsorption of inhibitors on the metal surface from acidic solution takes place spontaneously and obeys Langmuir adsorption isotherm. The standard free energy of adsorption indicates that the adsorption mechanism of the hydrazines was involves physical and chemical but predominant with chemical interactions.
- Three hydrazines derivatives act as mixed-type inhibitors with predominantly cathodic one.

References

1. Dafali A., Hammouti B., Touzani R., Kertit S., Ramdani A., Elkacemi K., *Anti-corros. Meth. & Mat.* 49 (2002) 96-104.
2. Thomas J. G. N., in: *Proceeding of the 5th European Symposium on Corrosion inhibitors, 5 SEIC, Ann. Univ. Ferrara, Italy* (1980) p.453.
3. Dafali A., Hammouti B., Mokhlisse R., Kertit S., Elkacemi K., *Corros. Sci.* 45 (2003) 1619–1630.
4. Donnelly B., Downier T.C., Grzeskowiak R., Hamburg H.R., Short D., *Corros. Sci.*18 (1977) 109.
5. Singh A. K., Quraishi M. A., *Corros. Sci.* 52 (2010) 152.
6. Fouda A. S., Al-Sarawy A. A., El-Katori E. E., *Desalination*. 201 (2006) 1.
7. Noor E. A., Al-Moubaraki A. H., *Mater. Chem. Phys*. 110 (2008) 145.
8. De Sauza F.S., Spinelli A., *Corros. Sci*. 51 (2009) 642.
9. Li, X., Deng S., Fu H., Li T., *Electrochimica Acta*. 54 (2009) 4089.
10. Li X., Deng S., Fu H., Mu G., *Corros. Sci.* 51 (2009) 620.
11. Popova A., Sokolova E., Christov M., *Corros. Sci.* 45 (2003) 33.
12. Zarrouk A., Zarrok H., Salghi R., Hammouti B., Bentiss F., Touir R., Bouachrine M., *J. Mater. Environ. Sci.* 4 (2) (2013) 177-192.
13. Rallas S., Gulerman N., Erdeniz, H., *Farmaco.* 57 (2002) 171–174.
14. Gursoy A., Terzioglu, N., Ouch, G., *Eur. J. Med. Chem.* 32 (1997) 753–757.
15. Rollas S., Kucukguzel, S.G., *Molecules.* 12 (2007) 1910–1939.
16. ASTM, G 31-72, *American Society for Testing and Materials, Philadelphia, PA*, 1990.
17. Tsuru T., Haruyama, S., Gijutsu, B., *J. Jpn. Soc. Corros. Eng*. 27 (1978) 573.
18. McCafferty E., Hackerman, N., *J. Electrochem.Soc.*119 (1972) 146.
19. Bastidas J.M., Polo J.L., Cano E., *J. Appl. Electrochem.* 30 (2000) 1173.
20. Bouyanzer A., Majidi, L., Hammouti, B., *Bull. Electrochem.* 22 (2006) 321.
21. Kim J., Lim, W., Lee, Y., Kim, S., Park, S.R., Suh, S.K., Moon, I., *Industrial and Engineering Chemistry Research.* 50 (2011) 8272.
22. Mansfeld F., Kending, M.W., Tsai, S., *Corrosion.*37 (1981) 301; *Corrosion*, 38 (1982) 570.
23. Pinto E.M., Soares,D.M., Brett, C.M.A., *Electrochim. Acta.* 53 (2008) 7460
24. Tang Y-M., Yang W-Z., Yin X-S., Liu Y., Wan R.,Wang J-T., *Mater. Chem. Phys.* 116 (2009) 479.
25. Kissi M., Bouklah M., Hammouti B., Benkaddour M., *Appl. Surf. Sci*. 252 (2006) 4190.
26. Benabdellah M., Touzani R., Dafali A., Hammouti B., El Kadiri S., *Materials Letters.* 61 (2007) 1197-1204.

27. Rochdi A., Kassou O., Dkhireche N., Touir R., El Bakri M., Touhami M.E., Sfaira M., Mernari B., Hammouti B., *Corrosion Science*, 80 (2014)442.
28. Zarrouk A., Dafali A, Hammouti B., Zarrok H., Boukhris S., Zertoubi M., *Int. J. Electrochem. Sci.* 5 (2010) 46-55.
29. Benabdellah M., Aouniti A., Dafali A., Hammouti B., Benkaddour M., Yahyi A., Ettouhami A., *Appl. Surf. Sci.* 252 (2006) 8341 – 8347
30. Domenicano A., Hargittai I., *Accurate Molecular Structures, Their Determination and Importance, Oxford University Press, New York* (1992).
31. Moretti G., Quartarone G., Tassan A., Zingales A., *Mater. Corros.* 45 (1994) 641.
32. Abiola O.K., Oforka N. C., *Mater. Chem. Phys.* 83 (2004) 315.
33. Solmaz R., Altunbaş, E., Kardaş G., *Mater. Chem. Phys.* 125 (2011) 796–801.
34. Ozcan M., Solmaz R., Kardas G., Dehri I., *Colloids Surf.* A 325 (2008) 57.
35. HongboF.,"*Synthesis and application of new type inhibitors", Chemical Industry Press, Beijing*.(2002) 166.
36. Solmaz R., *Corros. Sci.* 79 (2014) 169–176.
37. Solmaz R., *Corros. Sci.* 81 (2014) 75–84
38. Bouklah M., Ouassini K., Hammouti B., Elidrissi A., *Appl. Surf. Sci*. 250 (2005) 50-56.
39. Döner A., Solmaz R., Özcan M., Kardaş G., *Corros. Sci.* 53 (2011) 2902–2913.